European Journal of Chemistry

Check for updates

View Journal Online
View Article Online

Current advancements in CO_2 capture using graphene-based materials

Madushan Dhammika Gunarathna [1,*], Nimeshi Aviddika Abeysinghe [1], Ashan Sithija Wickramaarachchi [1], and Polegodage Dilushi Sureka Ruwan Kumari [2]

[1] *Department of Chemistry, Faculty of Science, University of Kelaniya, Kelaniya, 11300, Sri Lanka*
[2] *Department of Microbiology, Faculty of Science, University of Kelaniya, Kelaniya, 11300, Sri Lanka*

* *Corresponding author at: Department of Chemistry, Faculty of Science, University of Kelaniya, Kelaniya, 11300, Sri Lanka.*
e-mail: mdham191@kln.ac.lk (M.D. Gunarathna).

REVIEW ARTICLE

10.5155/eurjchem.15.3.302-306.2561

Received: 27 April 2024
Received in revised form: 28 June 2024
Accepted: 04 July 2024
Published online: 30 September 2024
Printed: 30 September 2024

KEYWORDS

Graphite
Monoliths
Mesopores
Micropores
Graphene oxide
Reduced graphene oxide

ABSTRACT

In 2023, global CO_2 emissions were 37.4 billion tonnes and a 1.1% increase compared to 2022. Although most countries try to decarbonize their economies, oil and gas supplied 52% of the world's energy needs in 2021, and by 2050 it will be 47%. Therefore, in the future, oil and gas will still account for a considerable percentage of the energy sector. However, the continuous release of CO_2 into the atmosphere at this rate can result in severe environmental problems. One of the promising approaches to address this issue is CO_2 capture. This captured CO2 can then be stored underground or used to produce commercially valuable products. In recent years, graphene-based materials have gained attention in CO_2 capture due to their interesting properties, such as high thermal stability and durability. This review focuses mainly on recently published articles on carbon capture using graphene-based materials.

Cite this: *Eur. J. Chem.* **2024**, *15(3)*, 302-306 **Journal website**: www.eurjchem.com

1. Introduction

Graphite is one of the well-known carbon allotropes and consists of sp^2 hybridized carbons arranged in six-membered hexagonal rings [1,2]. Graphite is a layered structure, and hundreds and thousands of carbon layers are arranged on top of each other [3]. A single layer of graphite is known as graphene. It was first extracted by Andre Geim and Konstantin Novoselov in 2004, and they won the Nobel Prize in 2010 for their discovery [4]. These two scientists removed some flakes from graphite using scotch tapes, and they observed that some of the flakes were thinner than the others, so they kept removing the flakes until they obtained flakes that were only one atom thick. Although graphite and graphene have the same atomic arrangement, changing the number of layers can change the properties of the material (*i.e.*, it has been observed that decreasing the number of layers increases the electrical conductivity and thermal conductivity) [5-7]. Graphene has been emerging as a potential candidate for CO_2 capture in recent years due to interesting properties such as high surface area, high thermal stability, higher mechanical strength, high chemical stability, high selectivity, *etc.* [8,9]. However, the production of single-layer graphene is difficult and expensive; therefore, most studies are conducted using graphene derivatives such as graphene oxide (GO) and reduced graphene oxide (RGO). In addition, it is well known that it is possible to incorporate other elements, such as nitrogen and sulfur, into graphene layers to synthesize different graphene derivatives. Researchers around the world have suggested different materials for CO_2 capture, such as zeolites, alumina-based compounds, metal-organic frameworks, metal oxides, *etc.* [10]. However, most of these materials have several drawbacks, such as high cost, limited adsorption capacity, poor thermal stability, etc. [11,12]. Existing CO_2 capture technologies can be classified into two types: (i) carbon capture and storage and (ii) carbon capture and utilization [13]. The first step of carbon capture is the separation of CO_2 from gas streams. Several techniques are used, such as solid adsorbents, solvent absorption, cryogenic separation, and metal-organic frameworks [11]. The most commonly used technique is the use of amine solutions (*i.e.*, monoethanolamine/MEA) to separate CO_2 [14]. However, most of these techniques have not met the expected carbon capture efficiency and are energy-intensive and expensive [15,16]. Therefore, it is necessary to optimize existing carbon capture technologies to make this technology more feasible. This review focuses on recent advances in CO_2 capture using graphene-based materials.

https://dx.doi.org/10.5155/eurjchem.15.3.302-306.2561

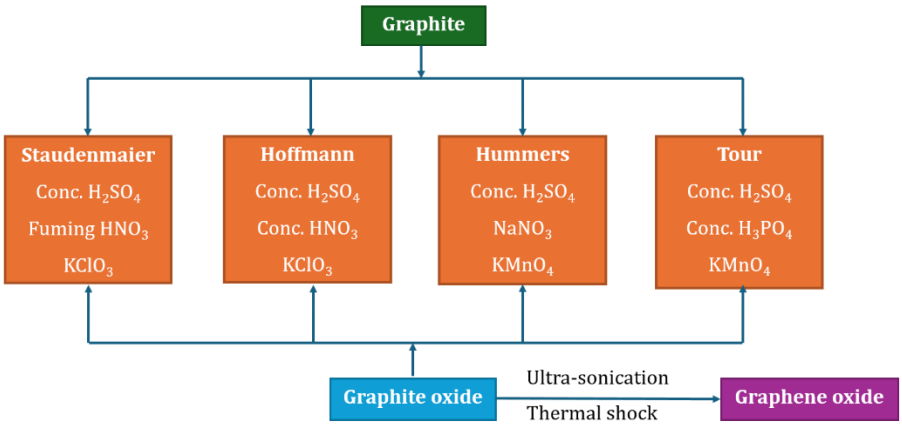

Figure 1. Various liquid phase processes which are used to synthesize graphene oxide from raw graphite.

2. Synthesis of graphene and graphene derivatives

Graphene can be synthesized using different methods such as chemical vapor deposition, electrochemical exfoliation, epitaxial growth, liquid phase exfoliation, mechanical exfoliation, and chemical exfoliation [17]. Out of these techniques, the most popular technique is liquid phase exfoliation due to its cost-effectiveness [18]. In liquid-phase exfoliation, intercalating agents are introduced into the graphite sheets, and these sheets are exfoliated. One of the popular liquid-phase exfoliation techniques is the modified Hummers method [19]. In the modified Hummers method, graphite is oxidized using an oxidizing agent in an acidic medium, and as a result, it will introduce oxygen functional groups (*i.e.,* epoxy groups, hydroxyl groups, and carboxylic acid groups) into the graphite layer. The introduction of oxygen functional groups increases the interlayer distance between graphite layers; hence, these graphite oxide layers can be separated by sonication, thermal shock, shearing, *etc.* [18]. Separated graphene oxide layers can be dissolved in water or any other suitable solvent due to the presence of functional oxygen groups [20]. Graphene oxide can be further reduced to form reduced graphene oxide using different reducing agents such as ascorbic acid (vitamin C), hydrazine hydrate, resveratrol, chitosan, polyethyleneimine, sodium borohydride, bovine serum albumin, green tea polyphenols, *etc.* [21,22]. As shown in Figure 1, there are some other liquid phase exfoliation methods, such as the Staudenmaier, Hofmann, and Tour methods [23]. Graphene oxide is commercially available now in different forms (*i.e.,* paste, powder, films, *etc.*), and there are leading suppliers such as Matexcel, CD bioparticles, Alfa Chemistry, ACS material, *etc.*

3. Graphene-based materials for CO_2 capture

An, L. *et al.* synthesized different types of nitrogen-rich porous carbons derived from graphene and tested them for their CO_2 adsorption capacity [24]. These nitrogen-rich porous carbons were synthesized using graphene oxide as the precursor. Graphene oxide was synthesized using the modified Hummers method and reacted with urea to incorporate nitrogen atoms, and this nitrogen-doped graphene was subjected to KOH activation [21]. Instead of urea, there are some other compounds that can be used as nitrogen doping agents, such as NH_3, ammonium salts, and nitric acid. KOH activation was carried out at different KOH concentrations and different activation temperatures to form different N-rich porous carbons [24]. As shown in Equations 1-4, during the KOH activation process, carbon atoms in nitrogen-doped graphene oxide react with KOH to form CO_2, CO, H_2, and carbonates [25]. This will create new voids in the structure and, as a result, will give rise to new micropores and mesopores; hence, it will significantly increase the surface area of BET (Brunauer, Emmett, and Teller) [26]. Micropores have a pore size of up to 2 nm, and pores in the range of 2 to 50 nm are classified as mesopores [27].

$$6KOH + 2C \rightarrow 2K + 3H_2 + 2K_2CO_3 \quad (1)$$

$$K_2CO_3 + 2C \rightarrow K_2O + 2CO \quad (2)$$

$$K_2CO_3 \rightarrow K_2O + CO_2 \quad (3)$$

$$2K + CO_2 \rightarrow K_2O + CO \quad (4)$$

Most of the studies have conducted BET surface area analysis (Brunauer-Emmett-Teller) and total pore volume analysis using nitrogen adsorption isotherms to study the textural properties of graphene-based materials. Nitrogen adsorption-desorption isotherms are graphs that are generated by measuring the volume of nitrogen adsorbed and desorbed onto a surface with respect to the relative pressure [28]. In the BET model, monolayer coverage is considered and uses the linear region of nitrogen isotherms, usually at relative pressures in the range of 0.05-0.35; this relative pressure range can also change depending on the type of adsorbent [29]. As shown in Figure 2, An, L. *et al.* measured the BET surface area of nitrogen-doped porous carbons derived from graphene in the relative pressure range P/P_0 = 0.04–0.32 [22].

Equation 5 represents the BET equation arranged in the y = mx + c format: V is the adsorbed gas quantity, P_0 is the saturation pressure of the adsorbate, P is the equilibrium pressure of the adsorbate, V_m is the monolayer adsorbed gas volume, C is the BET constant, E_1 is the heat of adsorption for the first layer, and E_L is the heat of vaporization. Equations 6-9 represent how to calculate the V_m using the slope and the intercept of the plot.

$$\frac{1}{V[(\frac{P_0}{P})-1]} = \frac{C-1}{V_m C}\left(\frac{P}{P_0}\right) + \frac{1}{V_m C} \quad (5)$$

$$C = \exp(\frac{E_1 - E_L}{RT}) \quad (6)$$

$$Slope = \frac{C-1}{V_m C} \quad (7)$$

$$Intercept = \frac{1}{V_m C} \quad (8)$$

$$V_m = \frac{1}{slope + intercept} \quad (9)$$

Table 1. CO_2 adsorption of T-GU-700-6, M90_0.5 and activated-RGO-950.

Material	Surface area (m^2/g)	Total pore volume (cm^3/g)	CO_2 uptake at 1 atm (mmol/g) 25 °C	0 °C	Isosteric heat of adsorption (kJ/mol)	Reference
T-GU-700-6	1032.00	0.82	2.40	3.24	-12-33	[24]
M90_0.5	328.00	1.35	2.10	-	-	[31]
Activated-RGO-950	1315.98	1.07	2.45	3.36	-27.42	[33]

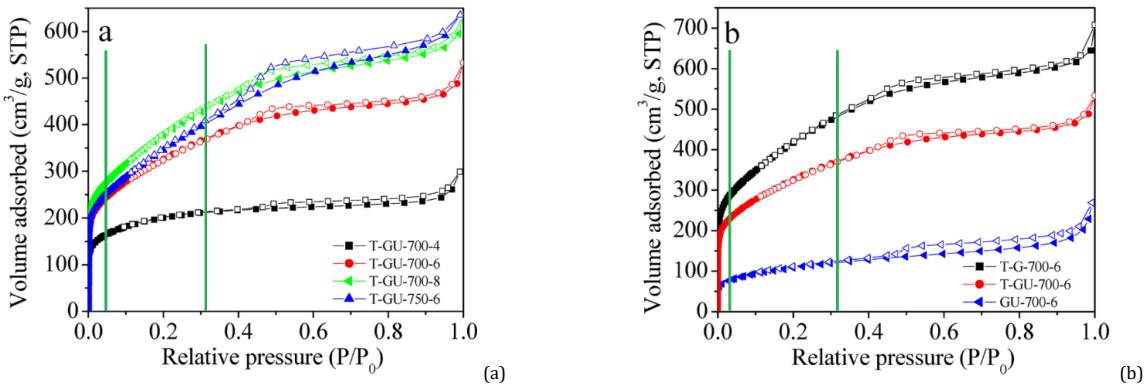

Figure 2. Nitrogen adsorption isotherms of nitrogen-doped porous carbons derived from graphene and the full green lines represent the approximate region that can be used for BET calculations *(images are adapted with permission from An, L. et al. Copyright (2019) American Chemical Society)* [24].

After evaluating the monolayer adsorbed gas volume (V_m), then Equations 10 and 11 can be used to get the BET surface area, where S_t is the total surface area of sample material, N is the Avogadro number, V is the molar volume of the adsorbed gas, s (0.162 nm^2) is the cross-sectional area of an adsorbed nitrogen molecule and a is the mass of the sample [30].

$$S_t = \frac{V_m N s}{V} \quad (10)$$

$$S_{BET} = \frac{S_t}{a} \ (m^2/g) \quad (11)$$

An, L. *et al.* reported that the thermal shocking process and KOH activation can increase the surface area of graphene-based materials [22]. However, increasing the temperature above a certain threshold level and continuously increasing the KOH concentration can decrease the surface area of graphene-based materials [22]. Politakos, N. *et al.* synthesized monolithic nanostructures from graphene oxide and reported that reduction of graphene oxide to a certain threshold level can increase the BET surface area of monolithic nanostructures [31]. Monoliths are structures consisting of pores that resemble a honeycomb [32]. Chowdhury, S. *et al.* synthesized graphene-based adsorbents using graphite as the starting material [33]. Graphite powder was used to synthesize graphene oxide, and graphene oxide was thermally reduced to form reduced graphene oxide. The reduced graphene oxide was physically activated by heating it to temperatures of 750, 850, and 950 °C in the presence of CO_2 flow (1000 mL/min) [30]. This physical activation process works in the same way as KOH activation, where CO_2 reacts with carbons in reduced graphene oxide sheets and produces gaseous species, as shown in Equation 12 [30]. As a result, it will increase the porosity of the material.

$$C + CO_2 \rightarrow 2CO \qquad \Delta H = 172 \text{ kJ/mol} \quad (12)$$

An, L. *et al.,* measured the CO_2 adsorption of different types of nitrogen-doped graphene synthesized under various conditions, and the highest CO_2 adsorption was observed in T-GU-700-6 [22]. T-GU represents the graphene oxide that reacted with urea after the thermal shock process, 700 is the activation temperature in Celsius during the KOH activation process, and 6 represents the ratio of KOH/T-GU [22]. Politakos, N. *et al.,* synthesized different monolithic nanostructures under various conditions and found that the highest CO_2 adsorption was seen in M90_0.5 [28]. M represents the monolithic nanostructure, 90 represents the temperature in Celsius at which the monolith was synthesized, and 0.5 represents the ratio of GO/ASA (Ascorbic acid/Vitamin C) ratio [28]. Studies by Chowdhury, S. *et al.* have shown that the highest CO_2 adsorption was seen for activated-RGO-950 [30]. 950 represents the temperature in Celsius at which the reduced graphene oxide was activated. Table 1 shows the CO_2 adsorption capacity, surface area, and isosteric heat of adsorption of these materials [24,31,33].

By comparing the values of CO_2 uptake of all materials in Table 1, it is clear that increasing the surface area does not significantly affect the CO_2 uptake. The highest total pore volume was observed for M90_0.5; however, CO_2 adsorption was lowest in M90_0.5; therefore, it is not possible to suggest that increasing porosity increases CO_2 adsorption. Comparing the textural properties of different materials from different studies on CO_2 adsorption is complex; therefore, evaluating the effect of surface area and total pore volume on CO_2 adsorption needs more studies. It is well known that gas adsorption decreases with increasing temperature; this can be seen here by comparing CO_2 uptake values at 25 and 0 °C; with increasing temperature, CO_2 adsorption has decreased [34]. The isosteric heat of adsorption is another important property that needs to be considered when studying gas adsorption because if an adsorbent has a very high isosteric heat of adsorption, it is difficult to desorb the adsorbed gas. If it has a very low isosteric heat of adsorption, it will decrease the CO_2 adsorption; therefore, moderate values are preferred. For physisorption processes, the isosteric values are generally between 5-40 kJ/mol [35]. The isosteric heat of adsorption values of T-GU-700-6 and activated-RGO-950 suggest that this is a physisorption process; however, no isosteric heat of adsorption values were given for M90_0.5.

An, L. *et al.,* N. *et al.,* and Chowdhury, S. *et al.* all have tested for the selectivity of CO_2 in the presence of N_2. T-GU-700-6, M90_0.5, and activated-RGO-950 had higher selectivity for CO_2 in the presence of nitrogen, as shown in Figure 3. However, none of these studies measured the selectivity of CO_2 in real flue gas conditions because the flue gas contains other species, such as O_2, SO_2, NO_x, and H_2O [36].

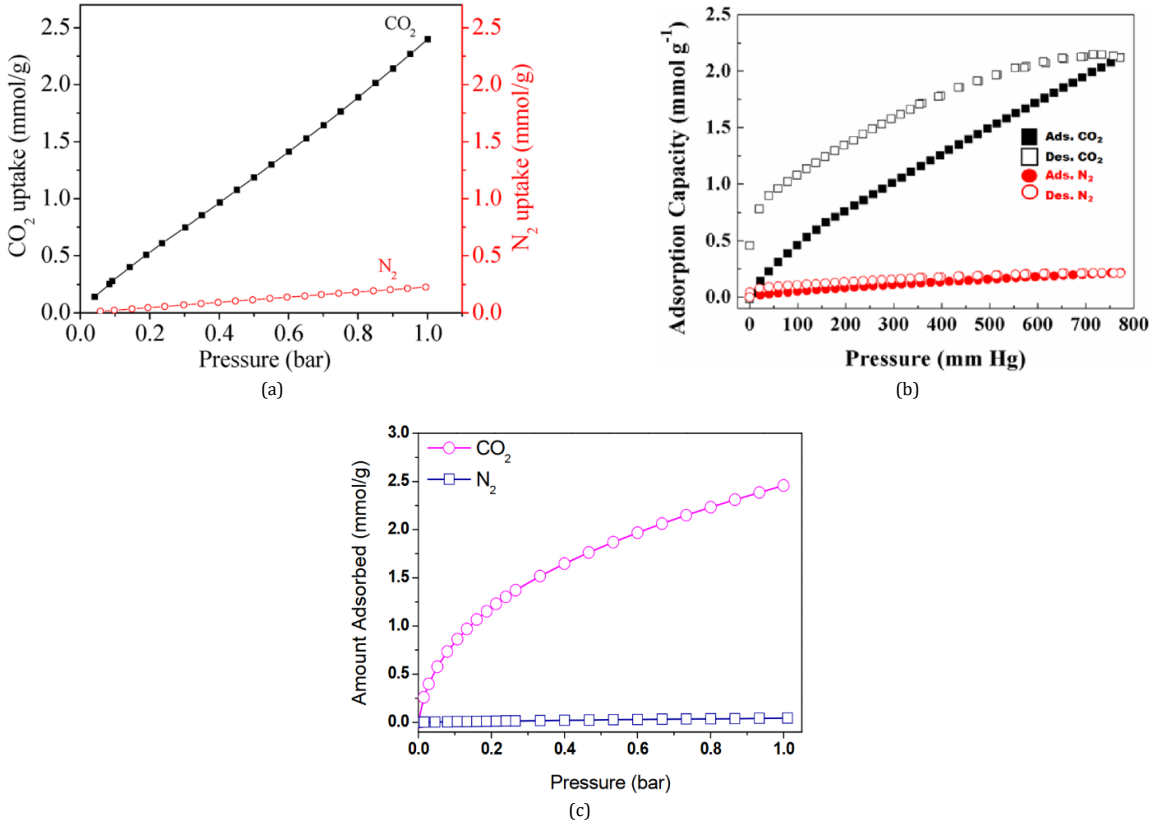

Figure 3. (a) CO_2 and N_2 adsorption of T-GU-700-6, (b) CO_2 and N_2 adsorption desorption of M90_0.5, and (c) CO_2 and N_2 adsorption of activated-RGO-950 *(Images are adapted with permission from An, L. et al. Copyright (2019) American Chemical Society Politakos, N. et al. Copyright (2020) American Chemical Society and Chowdhury, S. et al Copyright (2016) American Chemical Society)* [24,31,33].

In order to use these materials in the industry, their stability and recyclability must be tested. An, L. *et al.,* studied the cycle stability of T-GU-700-6 for five cycles and observed that there was only a 5% decrease in CO_2 adsorption compared to the first cycle [22]. Politakos, N. *et al.* studied the cycle stability of M90_0.5 for five cycles and reported that after each cycle there was a decrease in CO_2 adsorption; however, this decrease in CO_2 adsorption has slowly reduced with each cycle, suggesting that these monoliths are slowly stabilizing with respect to CO_2 adsorption [28]. Chowdhury, S. *et al.,* tested activated-RGO-950 for ten cycles and observed that there was no loss in CO_2 adsorption after ten cycles. Despite recent advances in developing novel materials derived from graphene for CO_2 capture, none of these materials have been commercially used so far. Therefore, more testing and research is needed to commercialize these graphene-based materials for CO_2 capture.

4. Conclusion

Different types of graphene-based materials were synthesized by An, L. *et al.,* Politakos, N. *et al.,* and Chowdhury, S. *et al.,* and CO_2 adsorption of all these materials was measured. Out of these studies, the highest CO_2 adsorption was seen for activated-RGO-950 at 25 °C and 0 °C. T-GU-700-6, M90_0.5 and activated-RGO-950 had higher CO_2 selectivity in the presence of nitrogen; however, all of these materials must be tested in real flue gas conditions. T-GU-700-6, M90_0.5, and activated-RGO-950 have shown the cycle stability and isosteric heat of adsorption values of T-GU-700-6 and activated-RGO-950 have shown that CO_2 adsorption is a physisorption process.

Acknowledgements

The authors would like to thank the Department of Chemistry, University of Kelaniya, for funding the publication of this paper.

Disclosure statement

Conflict of interest: The authors declare that they have no conflict of interest. Ethical approval: All ethical guidelines have been adhered.

CRediT authorship contribution statement

Conceptualization: Madushan Dhammika Gunarathna; Methodology: Madushan Dhammika Gunarathna, Nimeshi Aviddika Abeysinghe; Investigation: Madushan Dhammika Gunarathna, Ashan Sithija Wickramaarachchi; Resources: Madushan Dhammika Gunarathna, Ashan Sithija Wickramaarachchi, Nimeshi Aviddika Abeysinghe; Data Curation: Madushan Dhammika Gunarathna, Ashan Sithija Wickramaarachchi, Nimeshi Aviddika Abeysinghe, Polegodage Dilushi Sureka Ruwan Kumari; Writing - Original Draft: Madushan Dhammika Gunarathna; Writing - Review and Editing: Madushan Dhammika Gunarathna, Ashan Sithija Wickramaarachchi, Nimeshi Aviddika Abeysinghe, Polegodage Dilushi Sureka Ruwan Kumari; Visualization: Madushan Dhammika Gunarathna, Ashan Sithija Wickramaarachchi, Nimeshi Aviddika Abeysinghe, Polegodage Dilushi Sureka Ruwan Kumari; Supervision: Madushan Dhammika Gunarathna; Project Administration: Madushan Dhammika Gunarathna.

ORCID and Email

Madushan Dhammika Gunarathna
mdham191@kln.ac.lk
https://orcid.org/0009-0007-0262-0405
Nimeshi Aviddika Abeysinghe
nimeshiabeysinghe838@gmail.com
https://orcid.org/0009-0002-8526-9166

Ashan Sithija Wickramaarachchi
siwic1997@gmail.com
https://orcid.org/0000-0003-1654-2341
Polegodage Dilushi Sureka Ruwan Kumari
surekadilushi@gmail.com
https://orcid.org/0000-0001-6632-9034

References

[1]. Kharisov, B. I.; Kharissova, O. V. *Carbon allotropes: Metal-complex chemistry, properties and applications*; 1st ed.; Springer International Publishing: Basel, Switzerland, 2019.
[2]. *Synthesis and applications of nanocarbons*; Arnault, J.-C.; Eder, D., Eds.; John Wiley & Sons: Nashville, TN, 2020.
[3]. Okwundu, O. S.; Aniekwe, E. U.; Nwanno, C. E. Unlimited potentials of carbon: different structures and uses (a Review). *Met. Mater. Eng.* **2018**, *24*, 145–171.
[4]. Liu, Z.; Zhou, X. *Graphene: Energy storage and conversion applications*; CRC Press: London, England, 2021.
[5]. Sang, M.; Shin, J.; Kim, K.; Yu, K. J. Electronic and thermal properties of graphene and recent advances in graphene based electronics applications. *Nanomaterials (Basel)* **2019**, *9*, 374.
[6]. Terrones, M.; Botello-Méndez, A. R.; Campos-Delgado, J.; López-Urías, F.; Vega-Cantú, Y. I.; Rodríguez-Macías, F. J.; Elías, A. L.; Muñoz-Sandoval, E.; Cano-Márquez, A. G.; Charlier, J.-C. Graphene and graphite nanoribbons: Morphology, properties, synthesis, defects and applications. *Nano Today* **2010**, *5*, 351–372.
[7]. Zhang, L.; Deng, K.-K.; Nie, K.-B.; Wang, C.-J.; Xu, C.; Shi, Q.-X.; Liu, Y.; Wang, J. Thermal conductivity and mechanical properties of graphite/Mg composite with a super-nano CaCO3 interfacial layer. *iScience* **2023**, *26*, 106505.
[8]. Chin, B. L. F.; Loy, A. C. M.; Cheah, K. W.; Chan, Y. H.; Lock, S. S. M.; Yiin, C. L. Graphene-based nanomaterials for CO2 capture and conversion. In *Nanomaterials for Carbon Dioxide Capture and Conversion Technologies*; Elsevier, 2023; pp. 211–243.
[9]. Chowdhury, S.; Balasubramanian, R. Highly efficient, rapid and selective CO2 capture by thermally treated graphene nanosheets. *J. CO2 Util.* **2016**, *13*, 50–60.
[10]. Dziejarski, B.; Serafin, J.; Andersson, K.; Krzyżyńska, R. CO2 capture materials: a review of current trends and future challenges. *Materials Today Sustainability* **2023**, *24*, 100483.
[11]. Ozkan, M.; Custelcean, R.; Editors, G. The status and prospects of materials for carbon capture technologies. *MRS Bull.* **2022**, *47*, 390–394.
[12]. Makertihartha, I. G. B. N.; Dharmawijaya, P. T.; Zunita, M.; Wenten, I. G. Post combustion CO2 capture using zeolite membrane. In *AIP Conference Proceedings*; Author(s), 2017.
[13]. Leung, D. Y. C.; Caramanna, G.; Maroto-Valer, M. M. An overview of current status of carbon dioxide capture and storage technologies. *Renew. Sustain. Energy Rev.* **2014**, *39*, 426–443.
[14]. Luis, P. Use of monoethanolamine (MEA) for CO 2 capture in a global scenario: Consequences and alternatives. *Desalination* **2016**, *380*, 93–99.
[15]. Bae, J.; Chung, Y.; Lee, J.; Seo, H. Knowledge spillover efficiency of carbon capture, utilization, and storage technology: A comparison among countries. *J. Clean. Prod.* **2020**, *246*, 119003.
[16]. Hasan, S.; Abbas, A. J.; Nasr, G. G. Improving the carbon capture efficiency for gas power plants through Amine-based absorbents. *Sustainability* **2020**, *13*, 72.
[17]. Ikram, R.; Jan, B. M.; Ahmad, W. Advances in synthesis of graphene derivatives using industrial wastes precursors; prospects and challenges. *J. Mater. Res. Technol.* **2020**, *9*, 15924–15951.
[18]. Moosa, A. A.; Abed, M. S. Graphene preparation and graphite exfoliation. *Turk. J. Chem.* **2021**, *45*, 493–519.
[19]. Paramasivan, T.; Sivarajasekar, N.; Muthusaravanan, S.; Subashini, R.; Prakashmaran, J.; Sivamani, S.; Ajmal Koya, P. Graphene family materials for the removal of pesticides from water. In *A New Generation Material Graphene: Applications in Water Technology*; Springer International Publishing: Cham, 2019; pp. 309–327.
[20]. Neklyudov, V. V.; Khafizov, N. R.; Sedov, I. A.; Dimiev, A. M. New insights into the solubility of graphene oxide in water and alcohols. *Phys. Chem. Chem. Phys.* **2017**, *19*, 17000–17008.
[21]. Habte, A. T.; Ayele, D. W. Synthesis and characterization of reduced graphene oxide (rGO) started from graphene oxide (GO) using the tour method with different parameters. *Adv. Mater. Sci. Eng.* **2019**, *2019*, 1–9.
[22]. Banendu Sunder, D.; Gils, J.; Yu-Jen, L.; Jyh-Ping, C. Functionalized reduced graphene oxide as a versatile tool for cancer therapy. *Int. J. Mol. Sci.* **2021**, *22*, 2989.
[23]. Yokwana, K.; Ntsendwana, B.; Nxumalo, E. N.; Mhlanga, S. D. Recent advances in nitrogen-doped graphene oxide nanomaterials: Synthesis and applications in energy storage, sensor electrochemical applications and water treatment. *J. Mater. Res.* **2023**, *38*, 3239–3263.
[24]. An, L.; Liu, S.; Wang, L.; Wu, J.; Wu, Z.; Ma, C.; Yu, Q.; Hu, X. Novel nitrogen-doped porous carbons derived from graphene for effective CO2 capture. *Ind. Eng. Chem. Res.* **2019**, *58*, 3349–3358.
[25]. Raymundo-Piñero, E.; Azaïs, P.; Cacciaguerra, T.; Cazorla-Amorós, D.; Linares-Solano, A.; Béguin, F. KOH and NaOH activation mechanisms of multiwalled carbon nanotubes with different structural organisation. *Carbon N. Y.* **2005**, *43*, 786–795.
[26]. Harimisa, G. E.; Jusoh, N. W. C.; Tan, L. S.; Shameli, K.; Ghafar, N. A.; Masudi, A. Synthesis of potassium hydroxide-treated activated carbon via one-step activation method. *J. Phys. Conf. Ser.* **2022**, *2259*, 012009.
[27]. Storck, S.; Bretinger, H.; Maier, W. F. Characterization of micro- and mesoporous solids by physisorption methods and pore-size analysis. *Appl. Catal. A Gen.* **1998**, *174*, 137–146.
[28]. Lapham, D. P.; Lapham, J. L. Gas adsorption on commercial magnesium stearate: Effects of degassing conditions on nitrogen BET surface area and isotherm characteristics. *Int. J. Pharm.* **2017**, *530*, 364–376.
[29]. Marsh, H. Adsorption methods to study microporosity in coals and carbons—a critique. *Carbon N. Y.* **1987**, *25*, 49–58.
[30]. Dollimore, D.; Spooner, P.; Turner, A. The bet method of analysis of gas adsorption data and its relevance to the calculation of surface areas. *Surf. Technol.* **1976**, *4*, 121–160.
[31]. Politakos, N.; Barbarin, I.; Cantador, L. S.; Cecilia, J. A.; Mehravar, E.; Tomovska, R. Graphene-based monolithic nanostructures for CO2 capture. *Ind. Eng. Chem. Res.* **2020**, *59*, 8612–8621.
[32]. Govender, S.; Friedrich, H. Monoliths: A review of the basics, preparation methods and their relevance to oxidation. *Catalysts* **2017**, *7*, 62.
[33]. Chowdhury, S.; Balasubramanian, R. Three-dimensional graphene-based porous adsorbents for postcombustion CO2 capture. *Ind. Eng. Chem. Res.* **2016**, *55*, 7906–7916.
[34]. Guan, C.; Liu, S.; Li, C.; Wang, Y.; Zhao, Y. The temperature effect on the methane and CO2 adsorption capacities of Illinois coal. *Fuel (Lond.)* **2018**, *211*, 241–250.
[35]. Saffarionpour, S.; Tam, S.-Y. S.; Van der Wielen, L. A. M.; Brouwer, E.; Ottens, M. Influence of ethanol and temperature on adsorption of flavor-active esters on hydrophobic resins. *Sep. Purif. Technol.* **2019**, *210*, 219–230.
[36]. Zhao, Y.; Feng, D.; Li, B.; Wang, P.; Tan, H.; Sun, S. Effects of flue gases (CO/CO2/SO2/H2O/O2) on NO-Char interaction at high temperatures. *Energy (Oxf.)* **2019**, *174*, 519–525.